

Radiocarbon Dating, Chronologic Framework, and Changes in Accumulation Rates of Holocene Estuarine Sediments from Chesapeake Bay

Steven M. Colman, Pattie C. Baucom, and John F. Bratton

U.S. Geological Survey, 384 Woods Hole Road, Woods Hole, Massachusetts 02543

E-mail: scolman@usgs.gov

Thomas M. Cronin, John P. McGeehin, and Debra Willard

U.S. Geological Survey, National Center, Reston, Virginia 20192

Andrew R. Zimmerman

Virginia Institute of Marine Science, Gloucester Point, Virginia 23062

and

Peter R. Vogt

Naval Research Laboratory, Code 7420, 4555 Overlook Avenue SW, Washington DC 20375-5320

Received November 15, 2000; published online December 6, 2001

Rapidly accumulating Holocene sediments in estuaries commonly are difficult to sample and date. In Chesapeake Bay, we obtained sediment cores as much as 20 m in length and used numerous radiocarbon ages measured by accelerator mass spectrometry methods to provide the first detailed chronologies of Holocene sediment accumulation in the bay. Carbon in these sediments is a complex mixture of materials from a variety of sources. Analyses of different components of the sediments show that total organic carbon ages are largely unreliable, because much of the carbon (including coal) has been transported to the bay from upstream sources and is older than sediments in which it was deposited. Mollusk shells (clams, oysters) and foraminifera appear to give reliable results, although reworking and burrowing are potential problems. Analyses of museum specimens collected alive before atmospheric nuclear testing suggest that the standard reservoir correction for marine samples is appropriate for middle to lower Chesapeake Bay. The biogenic carbonate radiocarbon ages are compatible with ^{210}Pb and ^{137}Cs data and pollen stratigraphy from the same sites.

Post-settlement changes in sediment transport and accumulation is an important environmental issue in many estuaries, including the Chesapeake. Our data show that large variations in sediment mass accumulation rates occur among sites. At shallow water sites, local factors seem to control changes in accumulation rates with time. Our two relatively deep-water sites in the axial channel of the bay have different long-term average accumulation rates, but the history of sediment accumulation at these sites appears to reflect overall conditions in the bay. Mass accumulation rates at the two deep-water sites rapidly increased by about fourfold coincident

with widespread land clearance for agriculture in the Chesapeake watershed.

Key Words: Chesapeake Bay; estuaries; sediments; radiocarbon; Holocene.

INTRODUCTION

Holocene sediments deposited in estuaries offer many potential benefits as archives of paleoenvironmental information. Estuaries tend to act as traps for both fluvial and marine sediment and they typically accumulate sediment rapidly. High sedimentation rates offer great potential for high temporal resolution in proxy reconstructions. Estuaries are also sensitive physical and ecological systems that occur (by definition) at the interface between terrestrial and marine systems. As such, they respond dramatically to both natural climatic and geomorphic changes and to anthropogenic disturbances.

Compared with lacustrine and marine sediments, however, estuarine sediments have been relatively little used for paleoenvironmental reconstructions, especially on centennial to millennial time scales. Many of the problems that hamper paleoenvironmental reconstructions from estuarine sediments are the reverse sides of their advantages. For example, rapid sedimentation can make it difficult for common coring devices to reach the level of sediments deposited before anthropogenic influences. The deposition of sediments at the interface between marine and terrestrial

environments makes the sediments sensitive to change, but it also makes their interpretation complex. This complexity extends to a wide variety of sediment properties, including most proxies of past conditions, as well as materials for chronological studies. Of particular interest here, multiple sources of carbon in estuaries makes radiocarbon dating of the sediments difficult.

Chesapeake Bay is a classic coastal-plain estuary, the sediments of which represent well the general paleoenvironmental advantages and disadvantages of estuarine sediments. We address the problem of Holocene chronology in Chesapeake Bay by first comparing the radiocarbon ages of several fractions of the same samples and then by analyzing many samples in cores, as much as 20 m long, at each of six sites in the middle portion of the bay. Finally, we combine the radiocarbon ages with ^{210}Pb and ^{137}Cs data, pollen stratigraphy, and bulk density measurements to produce detailed age models and mass accumulation histories for selected sites. The age models we derive have two important functions: (1) they serve as the chronologic framework for all other estimates of past environmental conditions, and (2) changes in sediment accumulations rates are themselves indications of environmental conditions, especially for the post-European settlement period. These results have broad implications for the use of estuarine sediments as archives of paleoenvironmental conditions wherever thick estuarine sediments occur.

PREVIOUS WORK

For at least two reasons, relatively few radiocarbon ages have been obtained from sediments deposited in Chesapeake Bay. First, sediment accumulation rates are high in much of the bay, commonly more than 1 cm/yr (Officer *et al.*, 1984). Consequently, sediment accumulation rates for recent times are often better measured using ^{210}Pb and ^{137}Cs methods or pollen stratigraphy, and sediments from older periods generally are out of reach of common coring techniques. Second, carbon in Chesapeake Bay sediments occurs in a variety of forms, derived from many different sources, which creates difficulties in obtaining ages for specific sediment horizons. Thus, information on Holocene rates of sediment accumulation for centennial to millennial time scales in the bay previously have been essentially nonexistent.

Many studies have estimated sediment accumulation rates in Chesapeake Bay for the past 100–150 yr using radioisotope methods, especially ^{210}Pb (e.g., Goldberg *et al.*, 1978; Helz *et al.*, 1981; Officer *et al.*, 1984; Cornwell *et al.*, 1996; Zimmerman and Canuel, 2000). These studies show some coherent patterns, such as high rates in the upper and lower parts of the bay and lower rates in the middle. Many of the ^{210}Pb and ^{137}Cs profiles are complex, reflecting episodic deposition or process complexities on these time scales.

Several workers have carried out pioneering research using pollen stratigraphy linked to historical events for sedimentation chronology in Chesapeake Bay (Brush, 1984, 1986, 1989; Brush and Davis, 1984; Cooper and Brush, 1991, 1993; Cooper, 1995). Brush *et al.* (1982) also made direct comparisons between ages

estimated by ^{210}Pb and pollen-stratigraphy methods in the Potomac River estuary, a tributary of Chesapeake Bay. Donoghue (1990) reviewed many of the data related to sediment accumulation rates in the bay up to that date.

Despite this work on the uppermost sediments in the bay, no well-developed age models for Holocene sediments exist because of the general scarcity of radiocarbon determinations and uncertainty about the reliability of bulk organic carbon ages. We know of only three studies in the Chesapeake Bay area in which multiple radiocarbon ages have been determined in individual cores; none of these study sites are located in the open-water mainstem of the bay. The areas studied previously are in the estuarine parts of the Magothy River (Brush, 1986), the Rhode River (Donoghue, 1990), and the Potomac River (Glenn, 1984). A maximum of two dated cores, each with a maximum of three radiocarbon ages, were included in each study. In the latter study, ages based on wood samples were inconsistent with those based on total organic carbon.

METHODS AND DATA

Cores and Samples

Previous cores obtained for scientific purposes in the mainstem of the bay have been limited in length to about 5 m or less. Longer cores or boreholes have been obtained only from the fringing marshes and for the bridge and tunnel borings in the bay (Hack, 1957; Harrison *et al.*, 1964) and other engineering studies. In this study, we obtained and sampled several 4- to 5-m-long piston cores, along with ca. 1-m-long damped piston cores designed to recover the sediment–water interface. We also used a modified Mackereth corer to obtain cores with a composite length of almost 8 m (Table 1; Fig. 1). In addition, we sampled three of the Calypso cores from the 1999 cruise of the *R/V Marion-Dufresne*, cores that achieved lengths of as much

TABLE 1
Cores Sampled in This Study

Site	Core Name	Type	Latitude (°N)	Longitude (°W)	Water Depth (m)	Length (cm)
1	PTMC 3-2	Piston	38.0278	76.2202	23.1	450
1	MD99-2207	Calypso	38.0305	76.2147	23.1	2070
2	MD99-2204	Calypso	38.0527	76.2208	18.0	770
3	PX98-2	Piston	38.3311	76.3781	8.7	457
3	PX98-3	Damped Piston	38.3311	76.3781	8.7	97
4	PRCK 3-2	Piston	38.5439	76.4270	24.3	452
4	PR98-3	Damped Piston	38.5378	76.4296	21.9	97
4	PR98-4	Piston	38.5377	76.4299	21.9	427
5	RR98-4	Damped Piston	38.8776	76.4456	7.9	109
5	RR98-6	Long Piston	38.8776	76.4456	7.9	400
5	RR98-8	Mackereth	38.8783	76.4406	7.9	500
5	RR98-9	Mackereth	38.8789	76.4399	7.9	780
6	RD98-1	Piston	38.8867	76.3917	26.5	450
6	MD99-2209	Calypso	38.8867	76.3917	26.5	1720

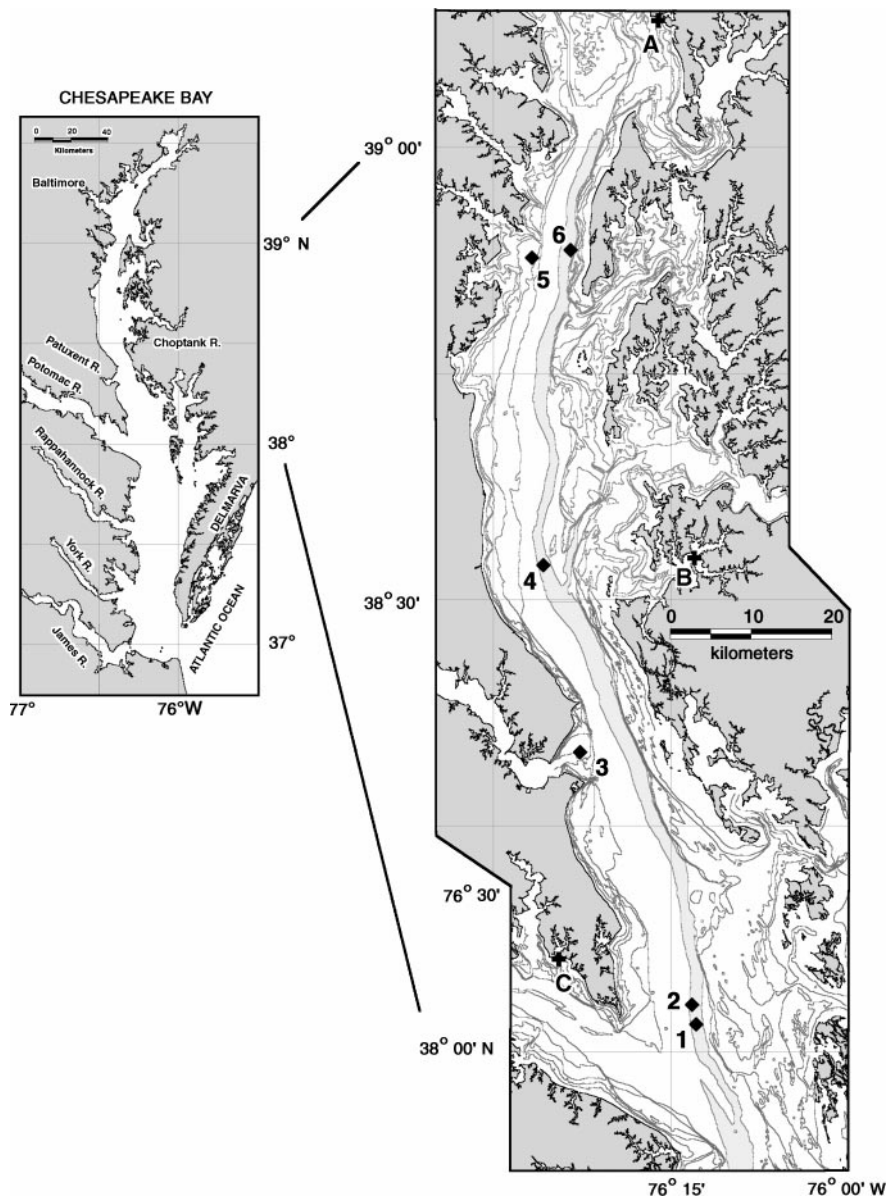


FIG. 1. Map of the mesohaline part of Chesapeake Bay showing cores sites (numbers, as in Table 1) and location of modern oyster samples (letters, as in Table 4). Bathymetric contours are at 6, 12, 18, 30, 36, and 60 ft.

as 20 m (Table 1; Fig. 1). Where multiple cores were collected at a single site, we assumed that they contained equivalent sections of sediment. This assumption was tested at sites 4 and 5 by correlating magnetic susceptibility profiles of individual cores (Baucom *et al.*, 2001). The results indicated that our assumption was valid, except for one of the Mackereth cores, in which a disturbed upper section was identified and corrected for using correlation to a stratigraphically overlapping adjacent core.

We analyzed a variety of sediment fractions by accelerator mass spectrometer (AMS) methods. Macroscopic shells were used when present. The shells mostly comprised relatively small clams (mostly *Mulinia lateralis*, *Macoma balthica*, and *Mya arenaria*). A few gastropod (*Anachis obesa*) and several speci-

mens of oyster (*Crassostrea virginica*) shells also were sampled and dated. In addition to bulk organic carbon, we analyzed the total carbon of samples that were prepared for pollen analyses following techniques described in Willard *et al.* (2000). Sample splits were also suspended and sieved, and the >63-micron size fraction was handpicked under a binocular microscope for datable material, such as foraminiferal tests, fish scales, and pieces of woody material.

Radiocarbon Analyses

Organic carbon samples were acidified with organic-free HCl and placed in reaction tubes along with 2 g of copper oxide and a

2-by-12-mm strip of silver foil. The tubes were evacuated, flame sealed, and then heated in a muffle furnace at 550°C for 5 h to convert organic carbon to carbon dioxide. Carbonate samples were cleaned, and where sample size permitted, rinsed with dilute, organic-free HCl. They were converted to carbon dioxide by dissolution in phosphoric acid.

Carbon dioxide from the samples was reduced to elemental graphite over hot iron in the presence of hydrogen (Vogel *et al.*, 1984). The graphite targets were prepared and analyzed at the NOSAMS facility in Woods Hole (OS numbers in Table 2), or they were prepared at the U.S. Geological Survey (WW numbers in Table 2) and run at the Lawrence Livermore Accelerator Facility (CAMS numbers in Table 2). Ages were calculated according to the methods of Stuiver and Polach (1977), using measured values of $\delta^{13}\text{C}$, although in a few cases, $\delta^{13}\text{C}$ values were assumed (Table 2). Calibrated ages were calculated with the CALIB 4.1 program (Stuiver *et al.*, 1998), using the terrestrial calibration data set for organic carbon samples and the marine calibration data set (with $\Delta R = 0$) for carbonate samples.

RESULTS

The carbon in Chesapeake Bay sediments comes from a variety of sources (Fig. 2), only some of which provide carbon of the same age as the sediment in which it was deposited. The two largest carbon fractions of the sediments are microscopic organic matter (both allochthonous and autochthonous) and micro- to macroscopic biogenic carbonate. Also present are occasional

pieces of wood, roots, and miscellaneous allochthonous organic matter. The organic (noncalcareous) carbon in the sediments is a mixture of material contributed to the bay from shoreline erosion, riverborn suspended sediment, organic matter produced in the water column (by algae and other phytoplankton, for example), and windborn organic matter such as pollen. Of these fractions, the material contributed by rivers and shoreline erosion is suspect because of the unknown time between its formation and its final deposition. This fraction may also contain coal from the watershed of the Susquehanna River. Both pollen and autochthonous (produced within the bay, e.g., phytoplankton) organic matter ought to be suitable for radiocarbon dating, but they are difficult to separate from the terrigenous organic matter.

Biogenic carbonate in the bay consists of foraminifera tests and ostracode shells, as well as shells of a variety of macroscopic mollusks, including clams, gastropods, and oysters. All of these taxa are benthic epifauna or infauna. Potential problems for radiocarbon dating include transportation and redeposition, burrowing, and reservoir effects from the water in which the shells formed. We examined the cores for evidence of discrete burrows before taking samples. Deep burrowing by clams whose shells we analyzed is not believed to be a problem in our data, but it is difficult to eliminate as a possibility.

We began our analyses by examining several organic carbon and carbonate fractions of samples from the two 1996 cores (PTMC 3-2 and PRCK 3-2). Comparisons among these different fractions form the basis of our evaluation of potential problems

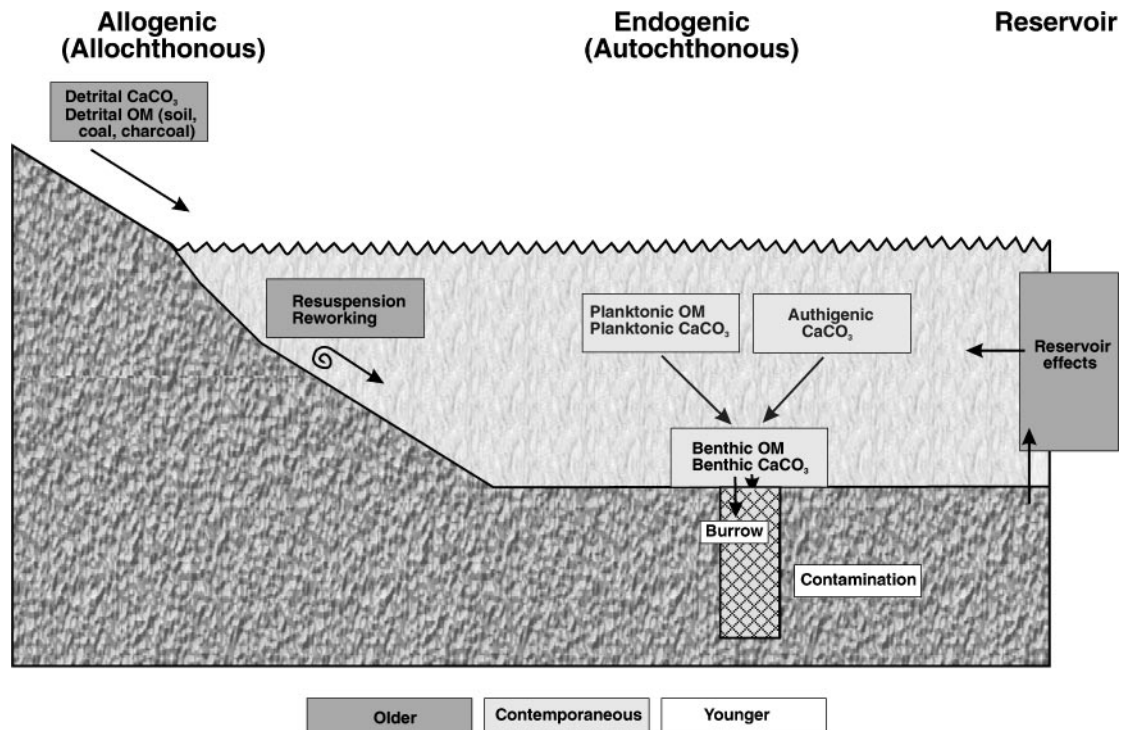


FIG. 2. Diagram showing the various sources of organic and inorganic carbon in the sediments of Chesapeake Bay. OM-organic matter.

TABLE 2
Radiocarbon Ages^a

Core	Depth (cm)	Depth Range ^b (cm)	Material ^c	Laboratory Number	$\delta^{13}\text{C}^d$ (per mil)	Age (¹⁴ C yr B.P.)	Error ^e (yr)	Cal age (cal yr B.P.)	(-) Cal Error ^f (yr)	(+) Cal Error ^f (yr)
Site 1										
PTMC-3-2	141.0	0.0	Shell	WW-1284 CAMS-39237	0.10	540	50	150	150	130
PTMC-3-2	225.0	3.0	Shell	WW-1589 CAMS43711	0.00	990	40	550	40	90
PTMC-3-2	410.5	3.5	Gastropod	WW-1285 CAMS-39238	0.10	1240	50	760	90	140
PTMC-3-A	81.0	1.0	Shell	OS-15679	0.01	540	30	150	150	110
PTMC-3-A	161.0	1.0	Shell	OS-15680	-0.29	885	35	500	50	40
PTMC-3-A	211.0	1.0	Shell	OS-15681	0.01	1150	25	675	25	45
PTMC-3-A	211.0	1.0	TOC	OS-18128	-22.36	2840	45	2940	140	130
PTMC-3-A	229.0	1.0	Forams	OS-17242	-1.72	1230	30	750	70	80
PTMC-3-A	297.0	1.0	Shell	OS-15689	0.10	1530	70	1060	140	170
PTMC-3-A	297.0	1.0	TOC	OS-18129	-22.56	3030	45	3210	130	140
PTMC-3-A	331.0	3.0	Forams	OS-17508	-2.41	2450	256	2080	550	630
PTMC-3-A	392.0	2.0	Forams	OS-17241	-1.94	2400	85	2000	180	270
PTMC-3-A	395.0	1.0	TOC	OS-18130	-22.36	3560	110	3840	280	310
MD99-2207	221.5	0.5	Shell	OS-21487	-0.42	855	25	490	40	20
MD99-2207	377.5	2.5	Shell	OS-25825	-2.04	125	50	0	100	100
MD99-2207	387.5	0.5	Shell	OS-21670	0.11	4100	45	4140	140	130
MD99-2207	573.5	0.5	Shell	OS-21671	-0.13	4470	45	4630	100	160
MD99-2207	687.5	2.5	Shell	OS-25826	0.14	4590	55	4810	180	120
MD99-2207	777.0	0.0	Shell	OS-21664	0.20	6130	55	6560	140	110
MD99-2207	833.5	0.5	Shell	OS-21665	0.18	6430	65	6900	160	180
MD99-2207	901.0	1.0	Shell	OS-25827	0.70	6540	45	7025	95	145
MD99-2207	901.0	1.0	Shell	OS-21666	-8.09	9150	65	9810	280	280
MD99-2207	960.0	0.0	Shell	OS-25828	-1.94	8150	55	8600	130	250
MD99-2207	993.0	0.0	Shell	OS-21667	0.37	7080	60	7560	110	90
MD99-2207	1152.5	2.5	Shell	OS-25829	-7.27	8930	65	9475	375	345
MD99-2207	1161.0	0.0	Shell	OS-21668	-9.66	9400	100	10,130	420	430
MD99-2207	1796.0	0.0	Wood	OS-21502	-27.78	38,500	780	NA	NA	NA
MD99-2207	1973.0	0.0	<i>Potamogeton</i> <i>sp. seed</i>	OS-30625	-17.49	10,400	70	12,340	560	500
MD99-2207	2051.0	0.0	Wood	OS-21503	-27.78	10,400	45	12,340	390	460
Site 2										
MD99-2204	407.0	1.0	Shell	OS-21669	-7.57	9350	70	10,000	290	300
MD99-2204	464.0	0.0	Shell	OS-21486	-10.62	9670	50	10,310	200	800
MD99-2204	544.0	0.0	Wood	OS-21504	-27.52	10,400	55	12,340	390	460
MD99-2204	626.0	0.0	Wood	OS-21501	-28.65	10,550	45	12,750	590	160
Site 3										
PX98-2	93.0	0.0	Shell	OS-18535	-1.37	580	35	250	130	30
PX98-2	106.0	0.0	Shell	OS-18661	-1.18	905	60	510	80	100
PX98-2	167.5	1.5	Shell	OS-20057	-0.41	860	40	480	60	50
PX98-2	198.0	0.0	Shell	OS-18534	-7.57	1210	45	730	70	120
PX98-2	381.0	0.0	Woody organics	OS-19852	-25.00	1500	35	1350	50	150
PX98-3	43.0	0.0	Shell	OS-18413	-5.35	780	40	430	110	50
PX98-3	72.0	0.0	Shell	OS-18411	-1.25	750	45	400	110	60
PX98-3	100.0	0.0	Shell	OS-18410	-0.91	675	45	290	40	130
Site 4										
PRCK-3-C	69.0	1.0	Shell	OS-15674	-0.14	1010	85	570	100	135
PRCK-3-C	79.0	1.0	Shell	OS-15676	-0.59	605	40	260	130	40
PRCK-3-C	139.0	1.0	Forams	OS-15675	-2.14	1220	80	740	110	180
PRCK-3-C	139.0	1.0	TOC	OS-18131	-22.73	2450	50	2470	120	240
PRCK-3-C	189.0	1.0	Forams	OS-15684	-2.10	1310	80	870	200	120

TABLE 2—Continued

Core	Depth (cm)	Depth Range ^b (cm)	Material ^c	Laboratory Number	$\delta^{13}\text{C}^d$ (per mil)	Age (¹⁴ C yr B.P.)	Error ^e (yr)	Cal age (cal yr B.P.)	(-) Cal Error ^f (yr)	(+) Cal Error ^f (yr)
PRCK-3-C	201.0	1.0	Forams	OS-15683	-2.08	1200	75	720	100	180
PRCK-3-C	229.0	1.0	Forams	OS-15677	-2.04	1190	70	710	90	180
PRCK-3-C	229.0	1.0	Forams, <i>E.e.</i>	OS-19508	0.00	1050	180	625	325	315
PRCK-3-C	229.0	1.0	Forams, <i>E.s.</i>	OS-17874	-2.54	1320	195	880	340	350
PRCK-3-C	289.0	1.0	Shell	OS-15682	-0.24	2100	80	1680	185	160
PRCK-3-C	309.0	1.0	Forams, <i>E.e.</i>	OS-17881	-2.18	2090	30	1660	100	60
PRCK-3-C	309.0	1.0	Forams, <i>E.s.</i>	OS-17884	-2.30	2090	55	1660	140	140
PRCK-3-C	319.0	1.0	Forams	OS-15686	-2.07	1290	75	830	160	130
PRCK-3-C	319.0	1.0	Shell	OS-15687	0.32	1850	80	1370	120	180
PRCK-3-C	319.0	1.0	TOC	OS-18132	-23.03	3470	55	3700	120	170
PRCK-3-C	339.0	1.0	Forams	OS-15685	-1.39	2090	70	1660	165	160
PRCK-3-C	349.0	1.0	TOC	OS-18133	23.00	4530	80	5150	270	300
PRCK-3-C	351.0	1.0	Fish scales	OS-17308	-23.94	3440	420	3690	940	1150
PRCK-3-C	351.0	1.0	Forams	OS-15690	-0.97	2570	70	2270	220	90
PRCK-3-C	409.0	1.0	Gastropod	OS-15678	-0.07	1130	80	660	120	170
PRCK-3-2	121.0	0.0	Shell	WW-1586	0.00	640	50	280	130	110
				CAMS-43708						
PRCK-3-2	259.5	2.5	Shell	WW-1587	0.00	1160	40	680	40	80
				CAMS-43709						
PRCK-3-2	368.0	2.0	Shell	WW-1588	0.00	1980	50	1520	120	120
				CAMS-43710						
PR98-3	57.0	0.0	Shell	OS-18409	-0.72	625	35	270	120	40
PR98-4	134.0	0.0	Shell	OS-18532	-1.04	535	35	140	140	120
PR98-4	166.0	0.0	Shell	OS-18660	-0.40	815	45	460	120	50
PR98-4	360.0	0.0	Shell	OS-18533	0.13	3030	35	2770	40	80
PR98-4	428.5	1.5	Forams	OS-21266	-0.81	3090	90	2850	140	250
PR98-4	434.0	0.0	Shell	OS-18662	-0.73	3360	100	3210	280	220
			Depth ^g							
				Site 5						
RR98-4	81.0	75.0	Shell	OS-18412	-2.68	1400	40	930	70	100
RR98-6	72.0	75.0	Shell	OS-18900	-3.36	1260	30	780	60	100
RR98-6	98.0	98.9	Shell	OS-18528	-2.97	1520	40	1050	90	100
RR98-6	167.0	162.4	Shell	OS-18524	-5.32	1750	35	1280	50	70
RR98-6	204.0	196.4	Shell	OS-18523	-2.43	1880	35	1400	70	100
RR98-6	246.0	235.0	Shell	OS-18902	-2.01	1970	30	1510	90	70
RR98-6	277.0	265.0	Shell	OS-18527	-1.79	2050	45	1600	100	110
RR98-6	285.0	273.0	Shell	OS-18901	-2.05	2030	35	1570	60	110
RR98-6	322.0	310.0	Shell	OS-18529	-2.29	2230	50	1820	120	110
RR98-6	344.0	332.0	Shell	OS-18526	-2.40	2290	35	1880	70	80
RR98-8	393.0	393.0	Shell	OS-21262	-3.14	2780	75	2480	140	220
RR98-8	536.0	536.0	Shell	OS-20056	-1.63	3760	55	3670	130	160
RR98-9	535.0	614.7	Shell	OS-20052	-1.30	4410	45	4530	110	160
RR98-9	570.0	648.8	Shell	OS-20054	-2.02	5240	55	5590	110	120
RR98-9	570.0	648.8	Oyster	OS-20053	-2.75	5340	40	5690	90	100
RR98-9	630.0	707.3	Oyster	OS-20055	-3.52	6060	55	6460	110	160
RR98-9	681.0	754.4	Woody organics	OS-26382	-23.93	6200	65	7090	110	160
RR98-9	698.0	775.3	Shell	OS-21270	-4.26	6850	110	7370	200	190
RR98-9	698.0	775.3	Woody organics	OS-20055	-28.09	6030	55	6820	90	190
RR98-9	722.0	799.3	Oyster	OS-25830	-4.66	7180	40	7640	70	60
RR98-9	770.0	847.3	Woody organics	OS-20055	-27.82	7940	45	8845	215	145
				Site 6						
RD98-1	92.0	0.0	Shell	OS-19213	-0.65	320	60	0	NA	NA
RD98-1	142.0	0.0	Shell	OS-19212	-0.04	325	60	0	NA	NA
RD98-1	203.0	0.0	Shell	OS-19216	-0.40	325	30	0	NA	NA

TABLE 2—Continued

Core	Depth (cm)	Depth Range ^b (cm)	Material ^c	Laboratory Number	$\delta^{13}\text{C}^d$ (per mil)	Age (¹⁴ C yr B.P.)	Error ^e (yr)	Cal age (cal yr B.P.)	(-) Cal Error ^f (yr)	(+) Cal Error ^f (yr)
RD98-1	274.0	0.0	Shell	OS-19940	-0.60	555	35	220	140	50
RD98-1	340.0	0.0	Shell	OS-19215	-0.87	725	55	340	70	120
RD98-1	457.0	0.0	Shell	OS-19214	-1.03	1150	85	675	125	195
MD99-2209	296.0	0.0	Shell	OS-21226	-0.87	610	30	270	120	30
MD99-2209	369.0	1.0	Shell	OS-21381	-0.57	745	35	410	100	40
MD99-2209	455.0	1.0	Shell	OS-21382	-0.68	1150	40	680	40	80
MD99-2209	485.0	1.0	Shell	OS-21227	-1.29	1240	30	770	60	100
MD99-2209	573.0	1.0	Shell	OS-21383	-0.90	1600	35	1165	95	65
MD99-2209	665.0	1.0	Shell	OS-21384	-1.73	2050	40	1610	90	90
MD99-2209	733.0	1.0	Shell	OS-21228	-0.77	2210	35	1810	90	70
MD99-2209	780.0	0.0	Shell	OS-21229	-0.74	2500	35	2140	70	140
MD99-2209	820.0	0.0	Shell	OS-21385	-0.18	4230	40	4340	130	80
MD99-2209	904.0	2.0	Shell	OS-21230	-0.70	5530	40	5905	95	85
MD99-2209	1029.5	0.5	Shell	OS-21231	-0.14	5690	40	6100	120	80
MD99-2209	1159.0	1.0	Shell	OS-21232	-0.08	5960	40	6380	90	60
MD99-2209	1199.0	1.0	Shell	OS-21233	0.02	5980	40	6390	90	70
MD99-2209	1439.0	1.0	Shell	OS-21488	-0.74	6250	35	6700	80	70
MD99-2209	1605.0	0.0	Shell	OS-21386	-3.73	6290	35	6730	80	100
MD99-2209	1694.0	0.0	Shell	OS-21489	-3.53	8670	45	9220	170	440
MD99-2209	1694.0	0.0	Oyster	OS-21387	-1.04	6660	45	7200	120	80
MD99-2209	1705.0	1.0	Shell	OS-21388	-1.49	7050	40	7550	100	43
MD99-2209	1720.0	0.0	Shell	OS-21389	-1.5a	7100	45	7570	70	80

^a All ages by accelerator mass spectrometer methods (see text). Calibrated (cal) ages calculated using CALIB 4.1 (Stuiver *et al.*, 1998).

^b Depth ranges given as plus and minus from midpoint; zero indicates single depth.

^c Material: TOC, total organic carbon; shell, small clams. See text for mollusk and foraminifera species (*E.s.* and *E.e.* indicate monospecific samples described in text).

^d $\delta^{13}\text{C}$ notation relative to Pee Dee Belemnite standard. Values of 0 and 25 are assumed; all others are measured.

^e One sigma.

^f Two sigma.

^g Equivalent depth in core RR98-8, from correlation of magnetic susceptibility profiles (Baucom *et al.*, 2001). Depth ranges for these samples is 0–1 cm from the midpoint depth.

related to the sources of carbon and our conclusions about the most reliable fraction for age estimates.

Organic Carbon

We analyzed the total organic carbon (TOC) of three samples, the total carbon of three samples that were prepared for pollen analysis, two samples of fish scales, and one sample of wood from the same horizons where small bivalves were collected and analyzed. A comparison of the organic carbon samples with biogenic carbonate samples from the same horizons (Fig. 3) shows that in all cases, the organic carbon samples yielded older ages than the carbonate samples. The difference is surprisingly systematic, amounting to 1500 to 2000 yr for most sample pairs. The similarity between the TOC and the pollen-preparation samples was somewhat unexpected, because the pollen-preparation procedures eliminate fine-grained and labile organic matter. However, this result is consistent with the observation of microscopic particles of coal or charcoal in the pollen-preparation samples. The unexpected result that the fish-scale samples were older than coexisting biogenic carbonate (and presumably older than the

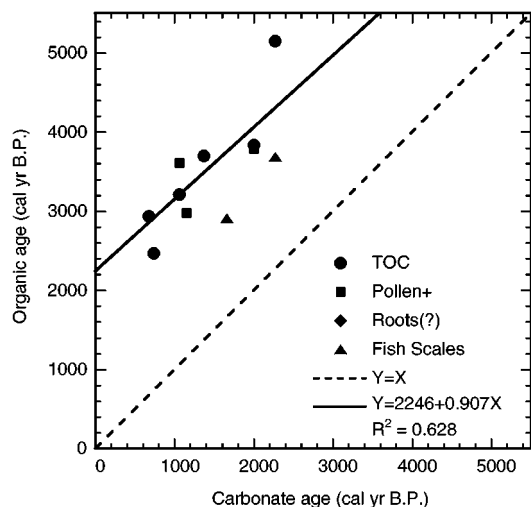


FIG. 3. Comparison between radiocarbon ages on carbonate and specified organic carbon fractions at the same horizons. One comparison of roots (6820 cal yr B.P.) with carbonate (7370 cal yr B.P.) (Table 2) is off the scale of the plot.

enclosing sediment) suggests that the fish scales were reworked before their final deposition.

Biogenic Carbonate

Among the foraminifera found in some intervals in the cores, two genera were commonly represented: *Ammonia* and *Elphidium*. Virtually all of the specimens that were handpicked for dating belonged to one of these two genera. Two species of *Elphidium* were observed: (1) *E. selseyense*, which is relatively small, yellowish, and shiny; and (2) *E. excavatum*, which is relatively large and chalky white. Although they have been identified as different species of *Elphidium* (Ellison and Nichols, 1976), they might be different ecophenotypes of the same species (Poag, 1978) or even specimens of the same species subjected to different amounts of transportation, reworking, or diagenesis. To test these possibilities, we separated the two groups in each of two samples and analyzed them separately (Table 3). The results indicate that the two groups are indistinguishable from each other by radiocarbon content. In fact, the fresher looking (shiny) group (*E. selseyense*) yielded a slightly older age in one of the two cases. These results support the interpretation that the two groups are either different species or ecophenotypes, rather than the same taxa subjected to different predepositional processes.

In addition to the foraminifera discussed above, biogenic carbonate samples from small clams (mostly *Mulinia lateralis*, *Macoma balthica*, and *Mya arenaria*), oysters (*Crassostrea virginica*), and gastropods (*Anachis obesa*) were analyzed. The two gastropod samples, one from the base of core PTMC-3 and one from the base of core PRCK-3, yielded anomalously young ages, at odds with the rest of the ages in the cores (Table 2). The ages of samples of oysters and foraminifera were compared with those of samples of clams from the same horizon (Fig. 4). Additional comparisons for these materials were generated by interpolating between closely spaced clam shell ages. No systematic differences appear among the fractions of biogenic carbonate (Fig. 4).

Reservoir Effects

Because biogenic carbonate in Chesapeake Bay is precipitated from seawater, the initial radiocarbon content of the shells is controlled by that of the dissolved inorganic carbon (DIC) pool at the site. Open ocean water typically has a ^{14}C deficit

TABLE 3
Comparison of Radiocarbon Ages ^{14}C yr B.P. of Two
Types of the Foraminifer *Elphidium*

Core, depth (cm)	<i>E. selseyense</i> (shiny, yellow)	<i>E. excavatum</i> (chalky, white)
PRCK-3C, 229	1320 ± 195	1050 ± 180
PRCK-3C, 309	2090 ± 55	2090 ± 30

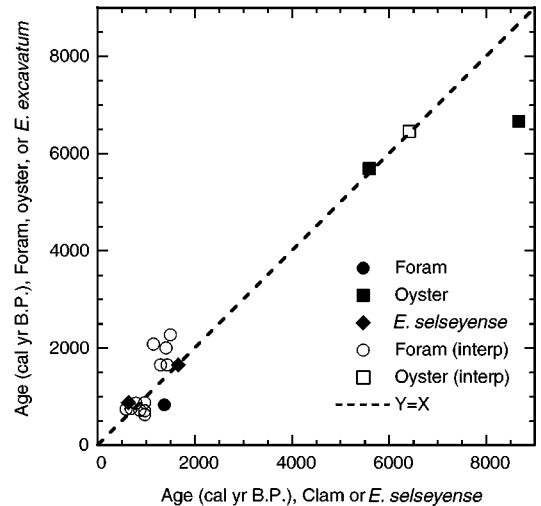


FIG. 4. Comparison between radiocarbon ages on clamshells and other carbonate fractions (foraminiferal tests and oyster shells) from the same horizons. In addition, a separate comparison between *Elphidium selseyense* and *E. excavatum* is shown, with *E. selseyense* on the abscissa. Open symbols indicate pairs for which the clam shell age was interpolated between closely spaced samples.

compared with the atmosphere, constituting a reservoir effect of about 400 yr (Stuiver and Reimer, 1993; Stuiver *et al.*, 1998). The reservoir correction for Chesapeake Bay may vary from the standard marine reservoir age of 400 yr because of mixing with river water in the estuary. Although oysters probably lived within a few meters of sea level, the other benthic organisms (clams, foraminifera) tend to live deeper, in contact with more marine water that bathes the estuary floor, whereas less dense river water remains near the surface.

To determine the appropriate correction for Chesapeake Bay samples, we analyzed three museum specimens of oysters (*Crassostrea virginica*) that were collected alive on known dates before atmospheric nuclear testing introduced artificial radiocarbon into the atmosphere and oceans. Radiocarbon ages for these samples are summarized in Table 4, along with the calculated reservoir effect. The results do not show a relation to distance from the mouth of the bay, and the average of 365 ± 143 yr is not significantly different from the standard marine correction of 400 yr. Consequently, the correction built into the CALIB 4.1 marine calibration set (with $\Delta R = 0$) was used when converting the radiocarbon ages of biogenic carbonate to calibrated or "calendar" ages. However, because of our small sample size (three) and the limited range of salinity variation (about 6–16‰) represented by the samples, more analyses of this type are needed.

The radiocarbon content of DIC in Chesapeake Bay water could also be affected by DIC diffusing from sediment pore water. If pore water DIC is derived from decomposition of recently deposited organic matter, it should have little effect on the radiocarbon content of the DIC of the water column. On the other hand, if there is a strong flux of pore water DIC to the water column, some of this carbon could be derived from deeper, older

TABLE 4
Collection Location of Museum Oyster (*Crassostrea virginica*) Specimens

Figure 1 symbol	Sample location	Lab no.	Year collected	$\delta^{13}\text{C}$ (per mil)	^{14}C age (^{14}C yr B.P.)	Expected age (yr B.P.) ^a	Reservoir effect
A	Swan Point (Kent County)	OS-22441	1818	-1.88	405 ± 30	79	326
B	Town Point (lower Choptank River)	OS-22440	1923	-4.32	385 ± 30	140	245
C	Smith's Creek (mouth of Potomac River)	OS-22439	1883	-1.56	610 ± 35	87	523

^a Expected age from tree ring data set (Stuiver *et al.*, 1998).

organic matter. In addition, a substantial amount of shell carbonate (as much as 50%) can be derived from metabolic carbon in some species, including *Mya arenaria* (Tanaka *et al.*, 1986).

Pore water DIC derived from decaying organic matter should have distinctively light $\delta^{13}\text{C}$ values because of the initial composition of TOC and the fractionation involved in diagenesis. Measurements of $\delta^{13}\text{C}$ and $\Delta^{14}\text{C}$ of the water column in Chesapeake Bay suggest that decomposition of suspended organic matter, not sedimentary organic matter, is the major source of DIC (Spiker, 1980) in the water column. $\delta^{13}\text{C}$ values for our carbonate samples mostly are close to zero (Table 2), although a few samples have $\delta^{13}\text{C}$ values as light as -10.6. Measurements on foraminifera that were not dated also range from 0 to -4 (J. F. Bratton, unpublished data, $n = 51$). The near-zero values are consistent with minor contribution of DIC from the diagenesis of sedimentary organic matter. Comparison of ages and $\delta^{13}\text{C}$ values of paired fractions of the same samples (Fig. 5) show little relation between the differences in ages and the differences in $\delta^{13}\text{C}$ values among the pairs. Nevertheless, a few samples with light $\delta^{13}\text{C}$ values seem anomalous, including two samples in Fig. 5 and an additional sample (RR98-9, 698 cm, Table 2) in which a shell with an $\delta^{13}\text{C}$ value of -4.26 is 550 yr older than woody organic material. So, pore water DIC derived from the

decomposition of organic matter appears to be a minor contributor to water column DIC and to the carbon in shells of benthic organisms, except possibly for a few samples, which could also be reworked. If old carbon dissolved in pore water makes a minor contribution to the radiocarbon content of benthic shells, either directly or through diagenesis, it would constitute a reservoir effect.

Reworking

Where sample ages form a systematic, monotonic series of increasing age with depth, we infer that reworking of older shells into younger sediments is not a significant problem. In most cases, the shells dated are relatively small, delicate clamshells that show no signs of abrasion or transport. In addition, *Mulinia* is a relatively short-lived, opportunistic, nonburrowing clam. However, oyster shells and the larger specimens of clams are relatively robust and capable of being transported and preserved intact. In some cases (Table 2), clam shell fragments were the only material available, and dating them increased the possibility of anomalously old ages. Reworking may be responsible for some of the scatter in ages in some cores (Fig. 6), especially in shallow-water, high-energy sites, although there is no simple relation to water depth. For example, site 5, in relatively shallow water, has little scatter in ages; this site was in a sheltered tributary channel until the channel was filled. Site 3 is in relatively deep water but has a large scatter in ages, possibly due to sediment mass movement on the edge of a channel. A few samples gave ages that are much older than those nearby and are thus clearly invalid (Fig. 6, sites 1 and 4). We infer that these anomalously old ages are due to shells that were transported and deposited with sediments younger than those in which the shells originally formed.

Conclusions Regarding Reliability of Ages

From the comparisons discussed above, we conclude that biogenic carbonate (clam shells and oysters shells and foraminiferal tests) provide the most reliable material for radiocarbon dating of Chesapeake Bay sediments. Some age uncertainties remain due to possible reworking of shell material and reservoir effects for samples in the bay. However, our results suggest that the standard open-ocean reservoir correction is approximately correct for these samples and that most cases of reworking can

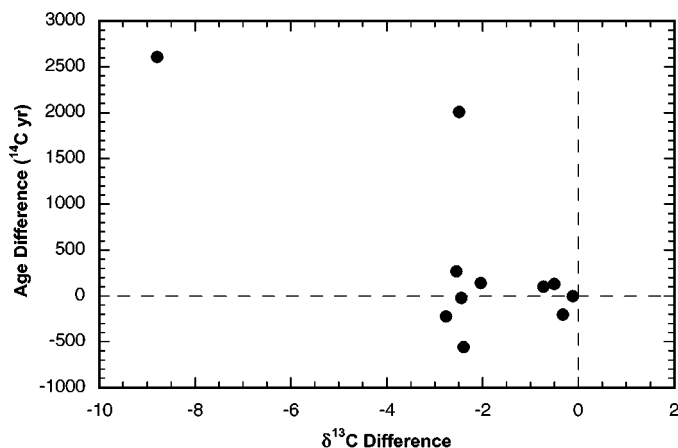


FIG. 5. Plot of $\delta^{13}\text{C}$ difference against age difference for carbonate sample pairs from the same horizon. For each pair, the isotope value and age of the sample with greater (heavier) $\delta^{13}\text{C}$ value (ranging from -2.18 to 0.70) was subtracted from those of the other sample. Data from Table 2.

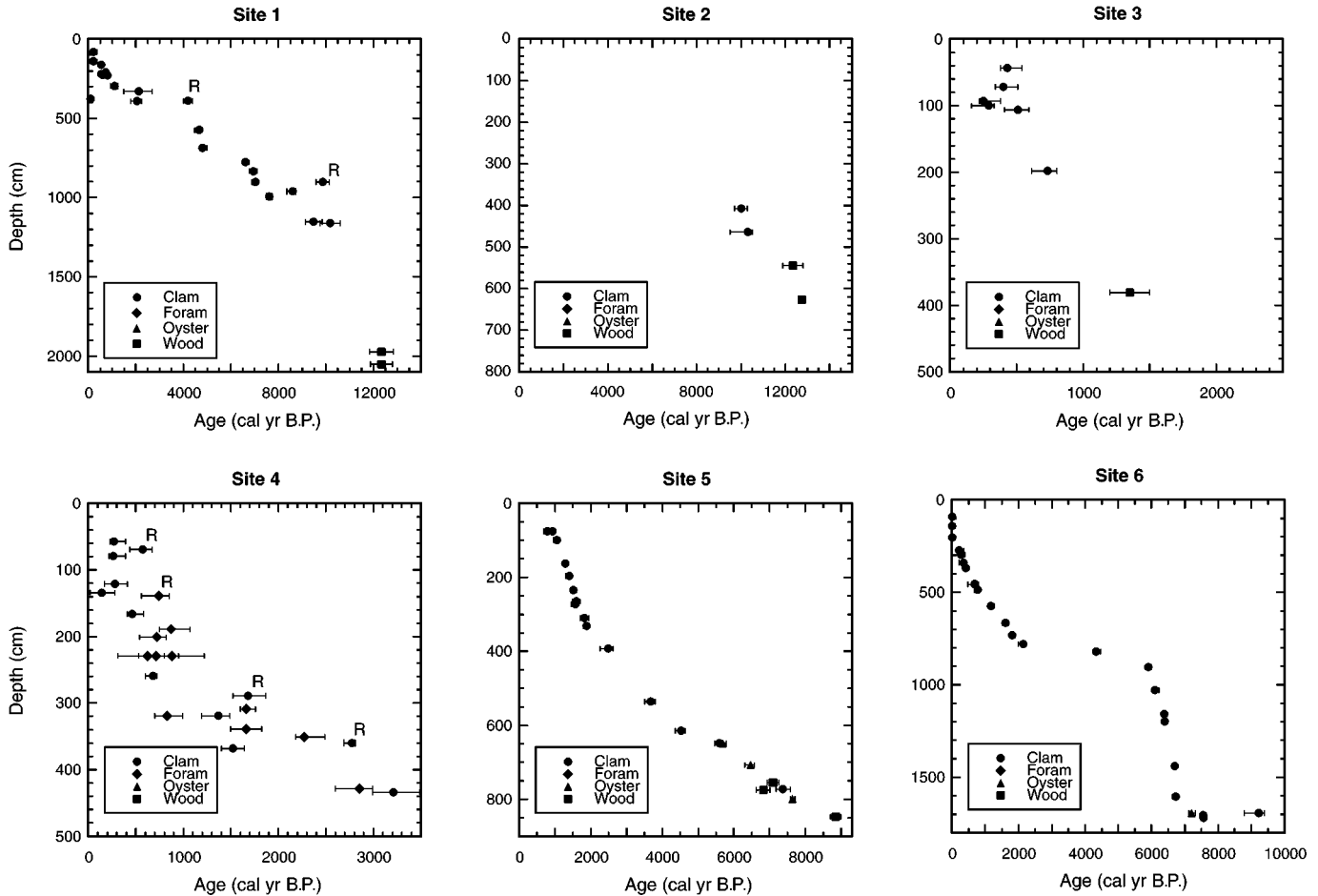


FIG. 6. Plot of radiocarbon ages against depth at each of the study sites. Data from Table 2. Samples labeled *wood* include macroscopic wood, roots, and seeds. R = samples suspected of being reworked.

be recognized. The results for samples of biogenic carbonate from each of the core sites are shown in Fig. 6. In some cases, wood produces apparently reliable ages, although the problem of transportation and redeposition is always a concern.

AGE MODELS FOR SELECTED SITES

The various reliability tests that were performed on the samples give us some confidence in using our results, combined with other age information, to construct age models for the sediments at selected core sites. We focus on the three sites with the longest records, two deep-water sites (1 and 6) from the axial channel of the bay and one (site 5) from a filled tributary channel. For each of these sites, the radiocarbon ages on carbonate were combined with radioisotope data (^{210}Pb and (or) ^{137}Cs) and pollen stratigraphic data. In all cases, the radioisotope and pollen data were compatible with the radiocarbon data on shells.

The ^{210}Pb and ^{137}Cs data for site 1 are from C. W. Holmes (in Cronin *et al.*, 1999) and that for sites 5 and 6 is from Zimmerman (2000). Interpretation of ^{210}Pb and ^{137}Cs profiles in terms of detailed chronology is extremely complex (Robbins and

Edgington, 1975; Oldfield and Appleby, 1984; Officer *et al.*, 1984). Here, we use ^{210}Pb and ^{137}Cs data only to estimate average rates of sediment accumulation over the last 100–150 yr (^{210}Pb) or 35 yr (^{137}Cs). Used this way, the ^{210}Pb and ^{137}Cs data are relatively robust and the uncertainties due to modeling of ^{210}Pb and ^{137}Cs distributions are relatively small, certainly smaller than the errors associated with a radiocarbon age.

Pollen stratigraphy and its relation to historical events have been used extensively in Chesapeake Bay (Brush, 1984, 1986, 1989; Brush and Davis, 1984; Cooper and Brush, 1991, 1993; Cooper, 1995; Cronin *et al.*, 2000; Willard *et al.*, 2000). Several events are identifiable in the record, but the most prominent is the rapid rise of *Ambrosia* (ragweed) pollen that accompanied land clearance for agriculture. This event occurred over a period of time, slightly different in different areas surrounding the bay. Rapid clearance of land began in the area in about 1780 (Brush, 1984) and peaked between 1840 and 1850 (Brush, 1989). We use a date of 1800 A.D. \pm 40 for the beginning of the rapid increase in *Ambrosia* pollen in our cores.

To eliminate the effects of compaction on sediment accumulation rates, we measured the water content of the sediments

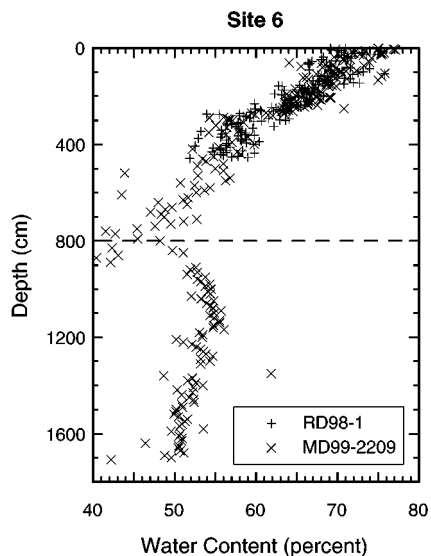


FIG. 7. Plot of water content against depth for cores RD98-1 and MD99-2209 at site 6. Note nonconformity at about 800 cm (see also Fig. 6).

and converted volumes (thicknesses per unit area) to masses. All water contents for our cores are tabulated in Baucom *et al.* (2001), and example data for site 6 are shown in Fig. 7. Assuming a solid particle density of 2.6 g/cm^3 and water density of 1.0 g/cm^3 (no correction for salt content), depth was converted to cumulative overlying sediment mass. Age was then plotted as a function of cumulative mass. Finally, a model curve was fit to the age-cumulative mass data using a locally weighted, least-

squares best fit method with smoothing factors of 0.33 to 0.50 (Fig. 8). Shell ages that appeared anomalously old, probably due to reworking as discussed previously, are indicated by question marks in Figure 8 and were not included in the model fit.

DISCUSSION

The data presented here provide the chronological framework for reconstructions of Holocene environmental conditions in the bay. These include salinity reconstructions in which changes are inferred to relate to climatically driven precipitation–streamflow changes (Cronin *et al.*, 2000).

In the longer cores, mass accumulation rates were relatively constant through much of the Holocene, at least for the fine-grained, open-estuarine deposits that overlie the basal, fluvial to restricted-estuarine units. The basal sediments commonly exhibit somewhat irregular ages, probably due either to irregular deposition and erosion or to reworking of the sediments and their shells.

Rates of sediment accumulation in Chesapeake Bay are spatially quite variable (Colman *et al.*, 1992). In a transverse direction, much of this variability is related to water depth and depositional environment, ranging from shallow-water, relatively high-energy nearshore environments to broad, moderate-depth shelves, to the relatively deep, partially filled paleochannels. Complicated wind- and tide-driven currents superimpose additional complexity on this pattern. The lowest overall variability in accumulation rates might be expected in the axial channel

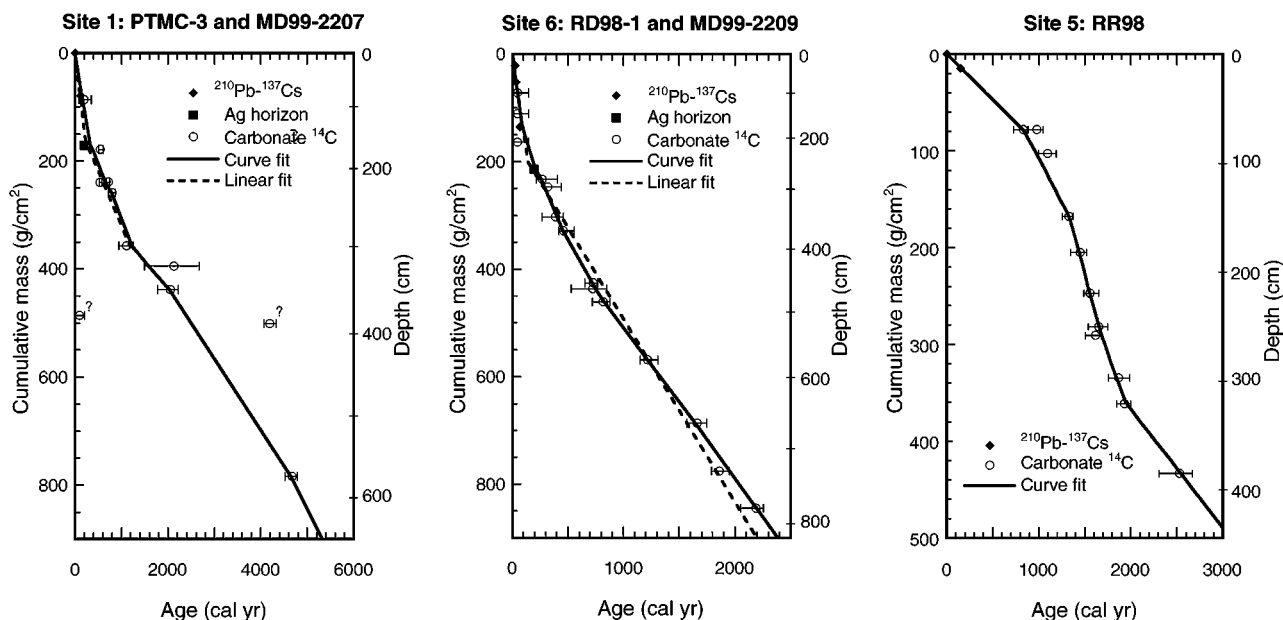


FIG. 8. Plot of radiocarbon and other age information against cumulative mass for the upper parts of the sections at sites 1, 5, and 6. Equivalent depths are on the right-hand ordinate. Solid curve is a local least-squares best fit to the data, excluding queried points (see text); dashed line is a two-line fit to the data. The time between 1950 A.D. and analysis of the samples has been added to the calibrated radiocarbon ages to make them compatible with the other data, hence they are not referenced as “B.P.”

TABLE 5
Comparison of Pre- and Post-1800 A.D. Accumulation Rates

Site	Mass accumulation rate (g/cm ² /yr)			Sedimentation rate (cm/yr)		
	Post-1800 A.D.	Pre-1800 A.D.	Ratio Post/Pre 1800 A.D.	Post-1800 A.D.	Pre-1800 A.D.	Ratio Post/Pre 1800 A.D.
1	0.717	0.201	3.57	0.691	0.145	4.76
2	ND	ND	ND	ND	ND	ND
3	0.247	0.425	0.58	0.192	0.326	0.59
4	0.045	0.213	0.21	0.050	0.219	0.23
5	0.100	0.094	1.06	0.100	0.090	1.11
6	1.429	0.340	4.20	1.786	0.277	6.45

ND = not determined.

of the bay, yet the paleochannel varies from nearly empty to completely full of Holocene sediment (Colman *et al.*, 1992).

To compare sedimentation rates before and after agricultural land clearance, we calculated rates of accumulation (both mass and thickness) before and after about 1800. Two straight lines were fit to the cumulative mass data, as shown in Fig. 8 for sites 1 and 6, and the same data were converted to depths to calculate sedimentation rates. These comparison reveal that two of the core sites show an increase in mass accumulation rate in their upper parts, whereas two others show a decrease in their youngest part and one shows little change compared with older sediments (Table 5). We infer that in many cases, changes in accumulation rate depend on local depositional environment, which is affected by water depth, sediment sources, and storm and tidal currents. An interesting example is provided by site 5 (Fig. 8), which is located in a filled tributary paleochannel in a present water depth of 7.9 m. The uppermost sediments at this site are coarser grained and accumulated more slowly than those below (Fig. 8). We infer that as the paleochannel filled relatively rapidly, the environment at the site became similar to that of the shallower water, higher energy, coarser grained sediments flanking the channel.

Many previous studies (references in Donoghue, 1990; Brush, 1989; Cooper and Brush, 1991, 1993; Cooper, 1995) have suggested that sediment accumulation rates in the bay increased during the last few hundred years, largely due to human settlement and land clearance. It has also been suggested that an increase in the rate of sea-level rise in the last few hundred years may have controlled accumulation rate (Donoghue, 1990). Our two sites from the axial channel of the bay (sites 1 and 6) each show a distinct increase in mass accumulation rate in the last 200–300 yr (Table 5; Fig. 8). We have modeled this change as a gradual transition, but two linear segments fit the data nearly as well (Fig. 8). The linear segments shown for sites 1 and 6 indicate about a fourfold (3.6 and 4.2) increase in mass accumulation rate in each case. The contrast in sedimentation rates before and after 1800 A.D. is even larger (Table 5).

Our two sites in the axial channel of the bay (sites 1 and 6) are 95 km apart and differ in average rate of mass accumulation by a factor of two. They maintain this ratio throughout their history, even as each shows an increase in rate of accumulation by a factor of four in the last 200 yr. The consistency of this fourfold increase between two sites in the simplest depositional setting, but which still differ in rate by a factor of two, strongly suggests that the fourfold increase in mass accumulation rate represents a large-scale (baywide) phenomenon. Although causality is difficult to prove, the change in mass accumulation rate is coincident with the history of land clearance and is plausibly related to it.

CONCLUSIONS

Two new advances have yielded the first long, well-dated Holocene sediment sequences from Chesapeake Bay: (1) long cores, several between 7 and 21 m long, which penetrate sediments older than a few hundred years in this high deposition rate environment; and (2) multiple AMS radiocarbon ages, which have allowed us to identify sediment components that yield reliable ages and to develop a sequence of ages in each core.

Biogenic carbonate (foraminiferal tests and mollusk shells) appears to be the most reliable sediment fraction for radiocarbon dating, although occasional cases of reworking of shells are apparent. Analyses of shells of oysters collected alive before 1950 suggest that the standard marine reservoir correction of about 400 yr is appropriate for the middle part of Chesapeake Bay.

Comparison of rates of accumulation among sites indicates large spatial variability of sedimentation rates in the bay, especially in relatively shallow-water environments. Two deep-water, axial-channel sites differ in rates of accumulation by a factor of two, but each shows a fourfold increase in the last 200–300 yr. This increase coincides with the increase in agriculture and land clearing in the watershed.

These results have several broad implications for estuarine studies. They form the chronological framework for a variety of paleoenvironmental reconstruction efforts in Chesapeake Bay using biological and geochemical proxies. In particular, our age models allow the calculation of fluxes, rather than just concentrations, of many constituents of the sediments through time. Development of these chronological and paleoenvironmental methods, in turn, contribute to the use of estuarine sequences in general as paleoenvironmental records.

ACKNOWLEDGMENTS

We thank several people for their help with the coring efforts including the late R. Kerhin and R. Younger, E. Mecray, D. Nichols, J. King, and C. Heil. King and Heil also shared their core-logging data with us. G. Rosenberg of the Philadelphia Academy of Natural Sciences kindly provided the samples of recently collected oysters. Helpful reviews were provided by L. D. Keigwin, C. W. Poag, D. B. Scott, and an anonymous reviewer.

REFERENCES

- Baucom, P. C., Colman, S. M., Bratton, J. F., Moore, J. M., King, J. W., Heil, C., and Seal, R. R., II. (2001). Descriptions and physical properties of selected cores collected in Chesapeake Bay in 1996 and 1998. U.S. Geological Survey Open-File Report 01-194, 113 pp.
- Brush, G. S. (1984). Patterns of recent sediment accumulation in Chesapeake Bay (Maryland—U.S.A.) tributaries. *Chemical Geology* **44**, 227–242.
- Brush, G. S. (1986). Geology and paleoecology of Chesapeake Bay: A long-term monitoring tool for management. *Journal of the Washington Academy of Sciences* **76**, 146–160.
- Brush, G. S. (1989). Rates and patterns of estuarine sediment accumulation. *Limnology and Oceanography* **34**, 1235–1246.
- Brush, G. S., and Davis, F. W. (1984). Stratigraphic evidence of human disturbance in an estuary. *Quaternary Research* **22**, 91–108.
- Brush, G. S., Martin, E. A., Defries, R. S., and Martin, C. A. (1982). Comparison of ^{210}Pb and pollen methods for determining rates of estuarine sediment accumulation. *Quaternary Research* **18**, 196–217.
- Colman, S. M., Halka, J. P., and Hobbs, C. H., III. (1992). Patterns and rates of sedimentation in Chesapeake Bay during the Holocene rise in sea level. In "Patterns and Rates of Sedimentation in Chesapeake Bay during the Holocene Rise in Sea Level" (C. Fletcher and J. F. Wehmiller, Eds.), pp. 101–111. Society of Economic Paleontologists and Mineralogists Special Publication No. 48.
- Cooper, S. R. (1995). Chesapeake Bay watershed historical land use: Impact on water quality and diatom communities. *Ecological Applications* **5**, 703–723.
- Cooper, S. R., and Brush, G. S. (1991). Long-term history of Chesapeake Bay anoxia. *Science* **254**, 992–996.
- Cooper, S. R., and Brush, G. S. (1993). A 2,500-year history of anoxia and eutrophication in Chesapeake Bay. *Estuaries* **16**, 617–626.
- Cornwell, J. C., Conley, D. J., Owens, M., and Stevenson, J. C. (1996). A sediment chronology of the eutrophication of Chesapeake Bay. *Estuaries* **19**, 488–499.
- Cronin, T., Colman, S. M., Willard, D., Kerhin, R., Holmes, C., Karlsen, A., Ishman, S., and Bratton, J. (1999). Interdisciplinary environmental project probes Chesapeake Bay down to the core. *EOS, Transactions of the American Geophysical Union* **80**, 237–241.
- Cronin, T., Willard, D., Karlsen, A., Ishman, S., Verardo, S., McGeehin, J., Kerhin, R., Holmes, C., Colman, S. M., and Zimmerman, A. (2000). Climatic variability in the eastern United States over the past millennium from Chesapeake Bay sediments. *Geology* **28**, 3–6.
- Donoghue, J. F. (1990). Trends in Chesapeake Bay sedimentation rates during the late Holocene. *Quaternary Research* **34**, 33–46.
- Ellison, R. L., and Nichols, M. M. (1976). Modern and itolocene foraminifera in the Chesapeake Bay region. Maritime Sediments Special Publication 1, pp. 31–151.
- Glenn, J. L. (1984). Sedimentation. In "A Water Quality Study of the Tidal Potomac River and Estuary—An Overview" (E. Callender, V. Carter, D. C. Hahl, K. Hitt, and B. I. Schultz, Eds.), pp. 39–41. U.S. Geological Survey Water Supply Paper 2233.
- Goldberg, E. D., Hodge, V., Koide, M., Griffin, J., Gamble, E., Bricker, O. P., Matisoff, G., Holdren, G. R., and Braun, R. (1978). A pollution history of Chesapeake Bay. *Geochimica et Cosmochimica Acta* **42**, 1413–1425.
- Hack, J. T. (1957). Submerged river system of Chesapeake Bay. *Geological Society of America Bulletin* **68**, 817–830.
- Harrison, W., Lynch, M. P., and Altschaeffl, A. G. (1964). Sediments of lower Chesapeake Bay, with emphasis on mass properties. *Journal of Sedimentary Petrology* **34**, 727–755.
- Helz, G. R., Sinex, S. A., Setlock, G. H., and Cantillo, A. Y. (1981). "Chesapeake Bay sediment trace elements." Research in Aquatic Chemistry Report, Dept. of Chemistry, University of Maryland, College Park, Maryland.
- Officer, C. B., Lynch, D. R., Setlock, G. H., and Helz, G. R. (1984). Recent sedimentation rates in Chesapeake Bay. In "The Estuary As a Filter" (V. S. Kennedy, Ed.), pp. 131–157. Academic Press, New York.
- Oldfield, F., and Appleby, P. G. (1984). Empirical testing of ^{210}Pb -dating models for lake sediments. In "Lake Sediments and Environmental History" (E. Y. Haworth and J. W. G. Lund, Eds.), pp. 93–124. Leicester Univ. Press, Leicester.
- Poag, C. W. (1978). Paired foraminiferal ecophenotypes in Gulf Coast estuaries: Ecological and paleoecological implications. *Transactions—Gulf Coast Association of Geological Societies* **28**, 395–421.
- Robbins, J. A., and Edgington, D. N. (1975). Determination of recent sedimentation rates in Lake Michigan using Pb-210 and Cs-137. *Geochimica et Cosmochimica Acta* **39**, 285–304.
- Spiker, E. C. (1980). The behavior of ^{14}C and ^{13}C in estuarine water: The effects of *in situ* CO_2 production and atmospheric exchange. *Radiocarbon* **22**, 647–654.
- Stuiver, M., and Polach, H. A. (1977). Discussion—Reporting ^{14}C data. *Radiocarbon* **19**, 355–363.
- Stuiver, M., and Reimer, P. J. (1993). Extended ^{14}C data base and revised CALIB 3.0 ^{14}C age calibration program. *Radiocarbon* **35**, 215–230.
- Stuiver, M., Reimer, P. J., and Braziunas, T. F. (1998). High-precision radiocarbon age calibration for terrestrial and marine samples. *Radiocarbon* **40**, 1127–1151.
- Tanaka, N., Monaghan, M. C., and Rye, D. M. (1986). Contribution of metabolic carbon to mollusc and barnacle shell carbonate. *Nature* **320**, 520–523.
- Vogel, J. S., Southon, J. R., Nelson, D. E., and Brown, T. A. (1984). Performance of catalytically condensed carbon for use in accelerator mass spectrometry. In "Proceedings of the 3rd International Symposium on Accelerator Mass Spectrometry" (W. Wolfi, H. A. Polach, and H. H. Anderson, Eds.), pp. 289–293. Nuclear Instruments and Methods in Physics Research B233.
- Willard, D. A., and Korejwo, D. (2000). Holocene palynology from *Marion-Dufresne* core MD99-2209, Chesapeake Bay. In "Initial Report on IMAGES V Cruise of the *Marion-Dufresne* to Chesapeake Bay June 20–22, 1999" (T. M. Cronin, Ed.), U.S. Geological Survey Open File Report 00-306, pp. 78–86.
- Zimmerman, A. R. (2000). "Organic matter composition of sediments and the history of eutrophication and anoxia in the mesohaline Chesapeake Bay." Unpublished Ph.D. dissertation, College of William and Mary, Williamsburg, VA.
- Zimmerman, A. R., and Canuel, E. A. (2000). A geochemical record of eutrophication and anoxia in Chesapeake Bay sediments: Anthropogenic influence on organic matter composition. *Marine Chemistry* **69**, 117–137.